

Research Article

Modeling and Simulation of Combined Heat and Mass Transfer in Zeolite SAPO-34 Coating for an Adsorption Heat Pump

Imen Amari ^{1,2} and M. H. Chahbani^{1,3}

¹Process Engineering and Industrial Systems Laboratory (LR11ES54), University of Gabes, 6072 Gabes, Tunisia

²National Engineering School of Gabes (ENIG), University of Gabes, 6072 Gabes, Tunisia

³Higher Institute of Applied Sciences and Technology of Gabes (ISSAT), University of Gabes, Gabes, Tunisia

Correspondence should be addressed to Imen Amari; imene.amarii@yahoo.com

Received 6 May 2021; Revised 22 August 2021; Accepted 8 September 2021; Published 30 September 2021

Academic Editor: Francisco Javier Fernández Fernández

Copyright © 2021 Imen Amari and M. H. Chahbani. This is an open access article distributed under the Creative Commons Attribution License, which permits unrestricted use, distribution, and reproduction in any medium, provided the original work is properly cited.

Heat and mass transfers inside an adsorbent bed of an adsorption heat pump (AHP) are considered poor; consequently, they can cause low system performance. They should be enhanced so as to increase the coefficient of performance of the cooling machine. The aim of this work is to study an adsorbent bed coated with the zeolite SAPO-34. A simulation model based on governing equations for energy, mass, and momentum transfers is developed using COMSOL Multiphysics software. The system zeolite SAPO-34/water has been considered. Modeling results are validated by experimental database available at the Institute for Advanced Energy Technologies “Nicola Giordano,” Italy. It has been shown that the adsorption heat pump performance is affected by both heat and mass transfer. The enhancement of heat transfer solely is not sufficient to attain high values of specific cooling power. In the case of water vapor/SAPO-34 pair, mass transfer has a significant impact on the duration of the cooling step which should be shortened if one would want to increase the specific cooling power. The sole way to do it is to enhance mass transfer inside porous adsorbent.

1. Introduction

Refrigeration and air conditioning systems are major consumers of electricity for heating and cooling demands [1]. These machines use CFCs for their operation which causes the depletion of the ozone layer [2]. In this context, the use of renewable energies as an alternative to fossil fuels is becoming increasingly essential [1, 3]. Nowadays, adsorption heat pump (AHP) has received much attention as a sustainable energy solution using environmentally friendly refrigerants such as water, methanol, and ammonia [4, 5].

The literature review showed that silica gel/water, activated carbon/methanol, activated carbon/ammonia, and zeolite (13X and 4A)/water are the most studied couples in the case of the adsorption heat pumps [6]. Wang et al. studied adsorption characteristics and the progress of the couple silica gel/water in adsorption refrigeration technologies [7, 8]. Interestingly, they found that the pair silica gel/

water is considered ideal for solar energy applications due to its low regeneration temperature. It requires a low-quality heat source, typically below 85°C. In addition, water has the advantage of having higher latent heat than other conventional refrigerants. It is suitable for air conditioning applications with high chilled water flows, where high evaporating temperatures can be used [7, 8]. Nevertheless, this pair has low adsorption capacity as well as low vapor pressure, which can limit mass transfer [9, 10].

The activated carbon/methanol is one of the most common working pairs in refrigeration adsorption systems. It also operates at low regeneration temperatures (care must be taken because regeneration temperatures above 120°C promote methanol decomposition), while its evaporative adsorption lift temperature is limited to 40°C [10]. In turn, the activated carbon/ammonia pair requires regeneration temperatures which can exceed 150°C. Its heat of adsorption is similar to that of the activated carbon/

methanol pair, but it requires higher operating pressures. Activated carbon/methanol pair leads to improving heat and mass transfer performance and shortens cycle time. All of these factors help to increase the specific cooling capacity of the system and make it even more attractive to researchers. However, activated carbon has a lower adsorption capacity for ammonia than methanol. In addition, care should be taken due to the toxicity of ammonia. It is very dangerous, forming an explosive mixture with air, and can form a certain chemical reaction with materials of construction of the machine such as copper [10, 11]. Cacciola and Restuccia compared the performances obtained from the regenerative cycles (heat pump or refrigeration system) for three pairs, zeolite 13X/water, zeolite 4A/water, and activated carbon AC35/methanol. They found that zeolite-water is the most suitable couple for making machines for use in domestic applications in southern European countries, where the market demand for devices, able to generate heat during the winter and cold during the summer, has been increased considerably [12]. Nonetheless, the pairs zeolite 13X/water and zeolite 4A/water have the disadvantage of requiring high regeneration temperature [6].

Considerable research activities on the development of new generations of porous materials for use in AHP were performed. In the last years, the silicophosphate SAPO-34 zeolite showed a high potential for cooling applications. The adsorbent material AQSOA-Z02, produced and developed by Mitsubishi Plastic Inc., is used as the commercial name for SAPO-34 [13].

Mitsubishi is a leading global manufacturer of high-performance thermoplastic materials. Heat conductivity, chemical resistance, and temperature resistance consist some of their specific topics in the focus of their current material development activities.

The compound zeolite SAPO-34 showed a high potential for cooling applications. Indeed, this adsorbent shows very suitable adsorption characteristics such as a high capacity of adsorption of water and typical conditions for adsorption cooling machines [13].

The enhancement of heat and mass transfers in adsorbers is a key factor for the development of adsorption heat applications. So, several concepts are proposed in innovative research to contact the adsorbent material with a metallic heat exchanger (HEX) [14].

- (i) Loose grain (granular)
- (ii) Consolidated
- (iii) Coated HEX

Santamaria et al. studied an adsorbent-HEX configuration with loose grains of AQSOA FAM-02 [15]. Aristov et al. optimized adsorption dynamics in adsorptive chillers with loose grains configurations [16]. Guilleminot et al. developed a new consolidated material made of metallic foam and zeolite [17]. Lang et al. investigated the adsorption rates of different compact zeolite layers for an adsorption machine [18]. The comparison of a consolidated adsorbent with an adsorbent of grains, made by Guilleminot

et al., demonstrates that the consolidated material has better heat transport characteristics than the granular adsorbent [17].

Publications about adsorbent developments for AHP showed that the main problem encountered in the design of consolidated and granular configurations is due to the highest heat and mass transfer resistances [19]. In order to overcome this issue, a coated adsorbent concept has been developed. Freni et al. tested a SAPO-34 coated adsorbent heat exchanger (Ad-HEX) [20]. Waszkiewicz et al. studied the performance of a coated finned tube of zeolite CBV901 [21]. Van Hayden et al. evaluated the performance of ALPO-18 coated-aluminum bed [22]. Freni et al. verified hydrothermal and mechanical stabilities of adsorbent coatings for AHP applications [23]. Okamoto et al. developed AQSOA-Z01, Z02, and Z05 coated heat exchangers for AHP [24]. Despite many advantages of the adsorption cooling machine, heat and mass transfers inside the adsorbent bed are considered poor; consequently, they can cause low system performance [5, 25, 26]. In order to overcome these issues, the coated heat bed, for adsorption cooling systems, showed very promising properties and better performances in terms of specific cooling power (SCP) [27].

The most common parameters used to evaluate the performance of an adsorption heat system are the coefficient of performance (COP) and the specific cooling power (SCP).

Melkon Tatlier investigated the specific cooling power (SCP) for different zeolite coatings. The power values obtained for zeolite NaX and zeolite LiX, were 0.69 kW/kg and 1.13 kW/kg, respectively [28]. Restuccia et al. performed a detailed study, realizing a solid adsorption chiller based on a heat exchanger coated with the Y type zeolite. The experimental results showed a SCP of 30–60 W/kg and a COP varies between 0.1 and 0.12 [29]. Suxin Qian et al. studied the performance of an adsorption chiller using a synthetic zeolite/water pair. In their study, the SCP of the cycle ranged from 0.1 to 0.9 kW/kg [30].

The objective of the present work is to investigate the coupled heat and mass transfer inside a cylindrical zeolite SAPO-34 coated bed numerically and experimentally. The performance of the adsorption bed is assessed through the evaluation of the parameters COP and SCP.

2. Mathematical Modeling: Governing Equations

The model under consideration has a cylindrical geometry (see Figure 1). Indeed, the compounds considered are as follows: the heating/cooling fluid (water), the metal tube, and the adsorbent bed zeolite SAPO-34 (AQSOA-Z02) which are all placed in a vacuum chamber.

The development of the mathematical model will be simplified by employing the following assumptions:

- (i) The adsorbent bed is composed of particles with identical properties and is uniformly distributed
- (ii) Densities, thermal conductivities, and specific heats for all materials are constant

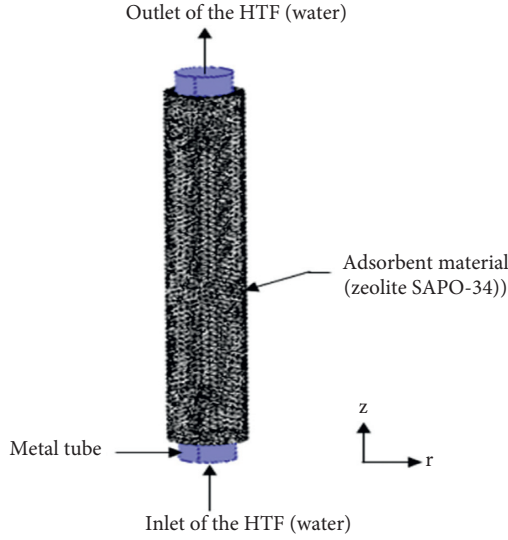


FIGURE 1: Schematic view of the cylindrical adsorbent bed.

- (iii) Heating/cooling fluid flows at a constant velocity within the tube
- (iv) Adsorbate vapor phase behaves as an ideal gas
- (v) Dynamic viscosity, permeability, total porosity, and heat of adsorption are taken as constant
- (vi) No heat losses are considered

2.1. Energy Conservation Equations. The energy balance for the circulating fluid (HTF) includes only energy transport by conduction and convection [31–33]:

$$k_f \nabla^2 T_f = \rho_f c_{pf} \frac{\partial T_f}{\partial t} + \rho_f c_{pf} \nabla_f \nabla T_f + \frac{2}{r_{ti}} h_i (T_f - T_t). \quad (1)$$

The energy equation for the metal tube including heat conduction is given by [34–36]

$$k_t \nabla^2 T_t + \frac{h_i A_{l,ti}}{V_t} (T_f - T_t) = \rho_t c_{pt} \frac{\partial T_t}{\partial t} + \frac{h_o A_{l,to}}{V_t} (T_t - T_s). \quad (2)$$

The energy equation for the adsorbent material has a complex form due to the three different phases: solid, adsorbate phases, and gas.

The energy balance for the porous media is written as [19, 32]

$$\begin{aligned} & (1 - \varepsilon) \rho_s c_{ps} \frac{\partial T_s}{\partial t} + \varepsilon \rho_v c_{p,v} \frac{\partial T_s}{\partial t} \\ & + (1 - \varepsilon) \rho_s X c_{p,l} \frac{\partial T_s}{\partial t} - (1 - \varepsilon) \rho_s |\Delta H| \frac{\partial X}{\partial t} \\ & - \varepsilon \frac{\partial P}{\partial t} - k_s \nabla^2 T_s + \rho_v c_{p,v} \cdot U \cdot \nabla T_s + \frac{h_o A_{l,to}}{V_s} (T_s - T_t) = 0. \end{aligned} \quad (3)$$

Adsorbate vapor phase (water vapor) behaves as an ideal gas and its equation of state is written as [37]

$$P = \rho_v R_v T_s. \quad (4)$$

2.2. Momentum Equations. For the mass momentum equation in porous media, the velocity of adsorbate gas, U , is considered in the radial and axial directions by using Darcy's equation [38, 39]:

$$\begin{aligned} u &= -\frac{\kappa}{\mu} \frac{\partial P}{\partial r}, \\ v &= -\frac{\kappa}{\mu} \frac{\partial P}{\partial z}, \end{aligned} \quad (5)$$

where κ is the bed permeability and evaluated by the following equation [38, 39]:

$$\kappa = \frac{d_p \varepsilon_b}{150(1 - \varepsilon_b)^2} \quad (6)$$

2.3. Mass Conservation Equation. The mass balance equation inside the adsorbent bed can be expressed as [19, 37]

$$\varepsilon \frac{\partial \rho_v}{\partial t} + (1 - \varepsilon) \rho_s \frac{\partial X}{\partial t} + \nabla(U \cdot \rho_v) = 0. \quad (7)$$

The amount adsorbed, X , can be calculated using the Linear Driving Force (LDF) model [38, 40]:

$$\frac{\partial X}{\partial t} = k_m (X_e - X), \quad (8)$$

where k_m is the internal mass transfer coefficient given by [38]

$$k_m = \frac{15}{r_p^2} D_{so} \exp\left(-\frac{E_a}{RT_s}\right). \quad (9)$$

The equilibrium adsorption capacity, X_e , of AQSOA-Z02 (SAPO-34)/water pair, is expressed by the Dubinin–Astakhov equation (see Table 1) [39, 41–43]:

$$X_e = X_o \exp\left(-\left(\frac{RT_s}{E} - \ln\left(\frac{P_{sat}}{P}\right)\right)^n\right). \quad (10)$$

P_{sat} defines the saturation pressure of water vapor inside the adsorbent bed [44]:

$$\ln(P_{sat}) = 25.1948 - \frac{5098.26}{T}. \quad (11)$$

2.4. Initial and Boundary Conditions. The temperature distribution for the HTF tube and the adsorbent bed are initially considered to be uniform as well as the adsorption capacity in the porous media:

TABLE 1: Parameter of Dubinin–Astakhov adsorption isotherm equation for AQSOA-Z02+ water pairs.

Isotherm equation	AQSOA-Z02+ water		
	X _o	E (J/mol)	n
Dubinin–Astakhov	0.31	7000	3

$$\begin{aligned}
 T_f(t=0, r, z) &= T_t(t=0, r, z) \\
 &= T_s(t=0, r, z) \\
 &= T_i, \\
 X(t=0, r, z) &= X_o, \\
 P(t=0, r, z) &= P_c.
 \end{aligned} \tag{12}$$

The boundary conditions for the heating/cooling fluid (HTF) and the tube are given as follows:

$$T_f(t, r, z=0) = T_h, \text{ during the heating process,}$$

$$T_f(t, r, z=0) = T_{co}, \text{ during the cooling process,}$$

$$\frac{\partial T_f}{\partial z}(t, r, z=L) = 0, \tag{13}$$

$$\frac{\partial T_t}{\partial z}(t, r, z=0) = \frac{\partial T_t}{\partial z}(t, r, z=L) = 0.$$

The boundary conditions for the adsorbent bed are as follows:

(i) Temperature boundary conditions:

$$\begin{aligned}
 \frac{\partial T_s}{\partial z}(t, r, z=0) &= \frac{\partial T_s}{\partial z}(t, r, z=L) \\
 &= \frac{\partial T_s}{\partial r}(t, r=r_b, z) \\
 &= 0,
 \end{aligned} \tag{14}$$

$$-k_s \frac{\partial T_s}{\partial r}(t, r=r_t, z) = h_o(T_t - T_{s|r=r_t}).$$

(ii) Pressure boundary conditions:

$$\frac{\partial P}{\partial r}(t, r=r_t, z) = 0,$$

$$\begin{aligned}
 P(t, r, z=0) &= P(t, r, z=L) \\
 &= P(t, r=r_b, z) \\
 &= P_c, \text{ when connected to the condenser,}
 \end{aligned}$$

$$\begin{aligned}
 P(t, r, z=0) &= P(t, r, z=L) \\
 &= P(t, r=r_b, z) \\
 &= P_e, \text{ when connected to the evaporator.}
 \end{aligned} \tag{15}$$

2.5. Performance Coefficients Equations. The performance of an adsorption heat pump can be measured by two coefficients: the coefficient of performance (COP) and the specific cooling power (SCP) [45]:

$$\text{COP} = \frac{Q_e}{Q_h}, \tag{16}$$

$$\text{SCP} = \frac{Q_e}{t_{\text{cyc}} * m_s}. \tag{17}$$

The cooling energy production in the evaporator, Q_e , can be calculated by the following expression:

$$\begin{aligned}
 Q_e &= \int_{t_{\text{cyc}12}}^{t_{\text{cyc}}} [L_v(T_e) - c_{pl}(T_c - T_e)] \cdot m_s \cdot \frac{\partial X}{\partial t} dt \\
 &= m_s \cdot \Delta X \cdot [L_v(T_e) - c_{pl}(T_c - T_e)],
 \end{aligned} \tag{18}$$

where

$$L_v(T) = L_o + \alpha_L \cdot T. \tag{19}$$

For the water vapor as adsorbate, $L_o = 3171.2$ kJ/kg and $\alpha_L = -2.4425$ kJ/kg·K [33].

The energy supplied to the adsorber during the heating period can be calculated from

$$Q_h = \int_0^{t_{\text{cyc}12}} h_o(T_t - T_{s|r=r_t}) dt. \tag{20}$$

3. Results and Discussion

3.1. Model Validation. The model relative to a coated bed of SAPO-34/water adsorption heat pump previously described in detail will be validated by comparing simulation results to ones from the experimental database available at the Institute for Advanced Energy Technologies “Nicola Giordano,” ITAE (CNR ITAE). An aluminum cylindrical tube is coated by the adsorbent material. The coating was prepared by dip-coating method starting from a water suspension of SAPO-34 zeolite and a silane-based binder.

The coating’s preparation and characterization were investigated according to the experimental testing method developed in [20]. Mechanical characterizations of the coatings were performed by a number of experimental protocols, conforming to [23].

Simulations have been achieved using the input data provided in Tables 2 and 3.

A two-dimensional axisymmetric geometry is considered. A time-dependent analysis of the coupled heat and mass transfer models has been performed using COMSOL Multiphysics software. In the simulation program, the heat transfer module for energy balances, chemical engineering module for mass balances, and partial differential equation (PDE) for the LDF module are chosen for the adaptation of governing equations.

The convection and conduction physics mode was selected to be the application module that describes heat transfer, respectively, in the HTF, metal tube, and the

TABLE 2: Main features of the coated adsorbent bed.

Heat transfer area (m ²)	0.94
Adsorbent content (kg)	0.084
Coating thickness (mm)	0.1
Sample with (%)	87.5 zeolite and 12.5 silane

TABLE 3: Thermophysical properties of the working pair and simulation parameters.

Parameter	Value	Unit	Source
C_{ps}	921	J/kg K	[39]
ρ_s	800	kg/m ³	[19]
k_s	0.3	W/m K	From experiment
d_p	100×10^{-9}	m	Fitting
E_a	44423.5	J/mol	[39]
D_{so}	1.97×10^{-10}	m ² /s	[20]
κ	5.00×10^{-12}	m ²	[19]
ΔH	3400	kJ/kg	[41]
ε	0.45	—	[46]
t_{cyc}	320	s	From experiment

adsorbent material as shown in equations (1)–(3). While convection and diffusion (equation (7)) were added to simulate the adsorption/desorption processes in micropores of sorbent particles via mass transport. Equation (8) was written as a differential equation and it can be introduced to COMSOL using a PDE form under COMSOL Multiphysics modules. Simulated configuration is meshed in COMSOL by using an extremely fine mesh to produce over 301846 triangular elements.

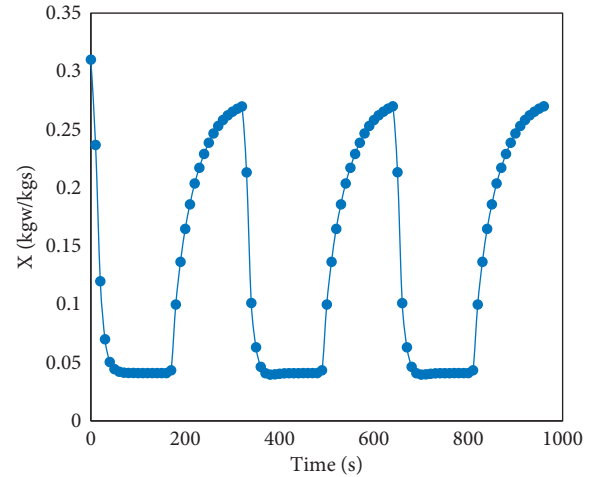
In order to enable high accuracy and convergence, solver settings of the COMSOL have the following properties:

- (i) Transient analysis type with ten seconds of step setting
- (ii) Direct impact method
- (iii) Relative tolerance: 0.1
- (iv) Absolute tolerance: 0.001
- (v) Stability of solution been set to automatic

Simulations are performed for adsorption and desorption processes.

Simulations are obtained for the following operating conditions: $T_i = 28.65^\circ\text{C}$, $T_h = 89.28^\circ\text{C}$, $T_{ev} = 8^\circ\text{C}$, $T_c = 28^\circ\text{C}$, and cycle time $t_{cyc} = 320$ s; they correspond to those used to get experimental database available at the Institute for Advanced Energy Technologies “Nicola Giordano,” ITAE (CNR ITAE) previously indicated.

The adsorbed amount variation with time, during the whole cycles (adsorption/desorption cycles), is shown in Figure 2. At the time $t = 0$ s, the adsorbed amount being at its maximum value, $X_o = 0.31$ kg_w/kg_s, begins to decrease when heating starts. For this heat transfer fluid temperature ($T_h = 89.28^\circ\text{C}$), it can be seen that SAPO-34 is nearly totally desorbed just after 50 s of heating during the desorption process. The bed becomes uniformly loaded without being completely desorbed. One has to increase the temperature of the heat transfer fluid to further reduce the amount adsorbed

FIGURE 2: Variation of average adsorption uptake (X) with time.

at the end of the heating step. The notable reduction of the duration of the heating step shows that the heat transfer between the adsorbent layer and the metal surface has been enormously enhanced by using the coating technique resulting in the obtention of a very reduced thickness ($r_b = 0.1$ mm).

Figure 3 shows a comparison between experimental and simulated average temperature evolutions of SAPO-34 coated bed during the adsorption/desorption process. It can be seen that the difference between the numerical results and experimental measurements in the adsorber is quite small. Therefore, the simulation results could be considered satisfactory insofar as the deviation between the two results does not exceed $\pm 2\%$. The simulation model could be used safely to predict system performance with high accuracy. One can note that, at $t = 60$ s and during the desorption cycle, the bed is totally heated and reaches almost the cycle maximum temperature of 362.43 K. Due to heat transfer enhancement induced by the coating reduced thickness, a heating duration of 60 s is sufficient and there is no need to extend the heating time beyond 60 seconds especially as the bed becomes uniformly desorbed as previously noted. The cooling duration should not be reduced because the bed takes more time to be totally saturated due to the reduction of the mass transfer rate in comparison to the one during heating (see Figure 2). The mass transfer rate is modeled herein by the Linear Driving Force (LDF) model. In fact, the values of diffusivities ($D_s = D_{so} \cdot \exp(-E_a/R \times T)$) of water vapor are 7.80×10^{-17} and 0.4×10^{-17} m²/s during heating ($T_h = 89.28^\circ\text{C}$) and cooling ($T_c = 28^\circ\text{C}$), respectively. The diffusivity is multiplied by nearly a factor of 20 when there is a 61°C temperature increase.

For adsorption heat pump applications, the coefficient of performance and the specific cooling power represent two important parameters to evaluate their performances.

Employing equations (16) and (17), the SCP and COP of the adsorbent material SAPO-34 (AQSOA-Z02) and water of an AHP are calculated and are summarized in Table 4.

For cycle time $t_{cyc} = 320$ s (160 s for heating and 160 s for cooling), COP and SCP values obtained by simulation are

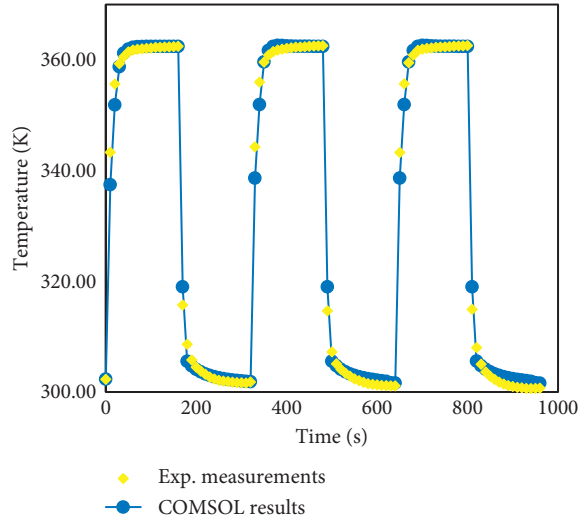


FIGURE 3: Variation of the average temperature in the adsorbent bed with time.

TABLE 4: Calculated COP and SCP for the SAPO-34 coated bed.

	COP	SCP (kW/kg)
SAPO-34 coated adsorbent bed	0.58	2.49

0.58 and 1.7 kW/kg, respectively. If the cooling time is taken equal to 60 s ($t_{cyc} = 220$ s) for the reasons given previously, the value of SCP obtained is 2.49, and COP remains unchanged (see Table 4). It can be noted that the coated adsorbent shows a good performance in terms of COP. On the other hand, it presents a high specific cooling power. For granular and consolidated beds, the values of COP are around 0.4 and 0.24, respectively [47], and the COP improvement is significant. Thus, the coated adsorbent bed seems to be a promising configuration for adsorption heat pumps technologies.

Table 5 illustrates a comparison of SCP values obtained in this study with those of some SAPO-34 coatings for adsorption heat pump reported in the literature.

In the following, after being validated, the simulation model will be used to assess the effect of the temperature of the heat transfer fluid and the evaporator pressure on the performance of the adsorption heat pump.

3.2. Effect of Heating Fluid Temperature. Variations with time of average temperature and adsorbed amount of water inside an adsorbent bed given by COMSOL simulations for the specified initial and boundary conditions are presented in Figures 4 and 5. All the results are obtained for the following operating conditions: $T_i = 28.65^\circ\text{C}$, $T_{ev} = 8^\circ\text{C}$, $T_c = 28^\circ\text{C}$, and cycle time (t_{cyc}) = 220 s. Three values of hot fluid inlet temperature were tested: $T_h = 89.28$, 120, and 150°C .

It is shown in Figure 4 that the adsorbent gets completely heated more rapidly when the temperature of the heat transfer fluid increases, and the bed temperature becomes

uniform in a shorter time. For the lower temperature of heat transfer fluid ($T_h = 89.28^\circ\text{C}$), the adsorbent bed reaches a uniform temperature after $t = 60$ s, whereas for the higher one ($T_h = 150^\circ\text{C}$), the heating is completed in 30 s. In other words, the cycle time of the system decreases with increasing the temperature of the heat source. Thus, this permits increasing COP and SCP of the system. It is worth noting that the choice of the temperature of heat transfer fluid is often imposed by some constraints related to the availability of the heat source. For example, if the adsorption heat pump is intended to be powered by solar energy, a temperature of 89°C seems to be suitable given the efficiency of solar collectors.

In Figure 5, it can be seen that the temperature of the heat transfer fluid has a significant influence on the desorption mass transfer rate during heating. As mentioned previously, when T_h increases, the diffusion coefficient of water vapor in the zeolite porous particles increases given its dependency with temperature resulting in a notable shortening of the desorption step. For $T_h = 150^\circ\text{C}$, the coated bed is completely desorbed in 20 s. For $T_h = 89.28^\circ\text{C}$, the coated bed could not be totally desorbed, nearly 15% of water vapor remains adsorbed in the bed at the end of the heating step regardless of the heating step time. This diminishes notably the system performance. In fact, the cooling energy production in the evaporator (Q_e) of the system, is directly related to the difference of water vapor adsorbed amounts at the end of cooling and heating steps. This difference in water vapor is cycled inside the adsorption heat pump flowing from the evaporator to the condenser and vice versa. One has to increase this difference for obtaining higher values of COP and SCP.

3.3. Effect of Evaporator Pressure. The transient variation of average temperature and average adsorbed amount inside the adsorbent bed for different values of P_e ($P_e = 0.8$, 1.053, and 1.228 kPa) for the specified initial conditions are shown in Figures 6 and 7, with $T_i = 28.65^\circ\text{C}$, $T_h = 89.28^\circ\text{C}$, $T_c = 28^\circ\text{C}$, and cycle time (t_{cyc}) = 220 s.

The three curves relative to the temperature variation with time for the different values of the evaporator pressure nearly coincide (Figure 6). It is clear that temperature inside the adsorbent bed is not affected by varying P_e as shown in Figure 6, despite the increase of the adsorbed amount as can be seen in Figure 7.

In fact, from Figure 7, it is found that increasing the evaporator pressure has a noticeable effect on the SAPO-34 uptakes. The highest value for adsorbed amount is obtained for the highest value of P_e as can be predicted by the Dubinin–Astakhov equation.

Due to the variation of the adsorbed amount, the coefficient of performance (COP) and the specific cooling power (SCP) of the couple SAPO-34/water are affected by varying P_e , as shown in Figure 8. The COP values vary from 0.521 for $P_e = 0.8$ kPa to 0.622 for $P_e = 1.228$ kPa. The corresponding values of SCP are 2.24 kW/kg and 2.68 kW/kg. Hence, as the evaporator pressure increases, the COP and SCP of the system increase. However, there is no significant

TABLE 5: Comparisons of SAPO-34 (AQSOA-Z02)/water pairs.

Ref.	Working pairs	Testing conditions ($T_h/T_c/T_i/T_{ev}$)	Coating thickness (m)	SCP (W/kg)
[20]	SAPO-34/water	90/28/28/15°C	100×10^{-6}	675
[48]	SAPO-34/water	90/21/39.8°C	45×10^{-6}	770
[49]	AQSOA-Z02/water	90/30/30/15°C	330×10^{-6}	250–480
—	Present study	89.28/28/28.65/8°C	100×10^{-6}	2.49×10^3

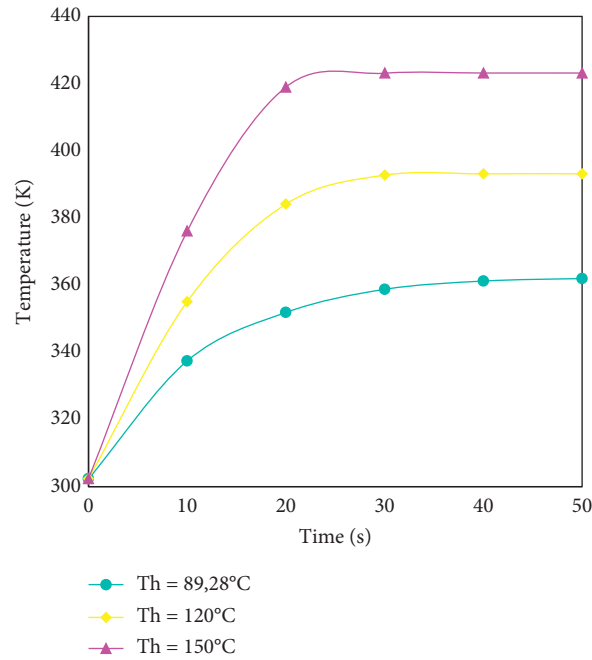


FIGURE 4: Variation of average bed temperature with time for different T_h .

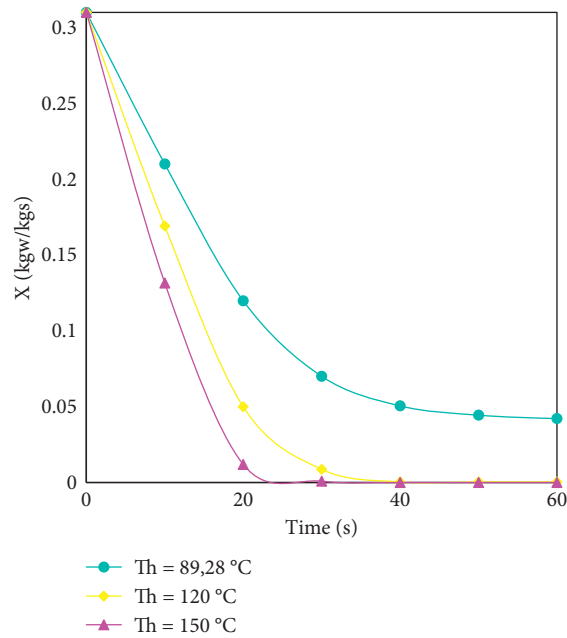


FIGURE 5: Variation of average adsorbed amount with time for different T_h .

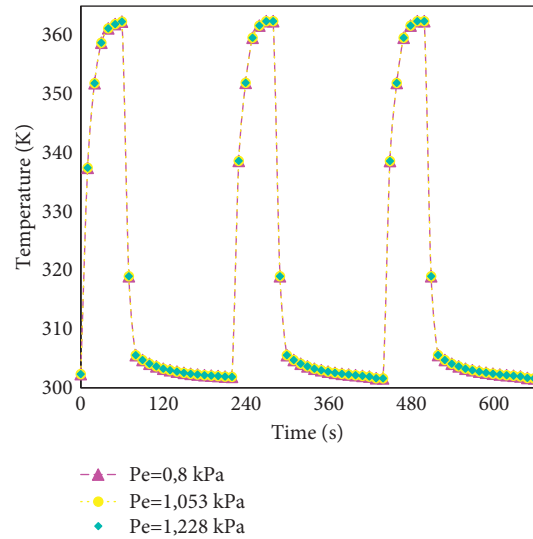


FIGURE 6: Variation of average bed temperature with time for different P_e .

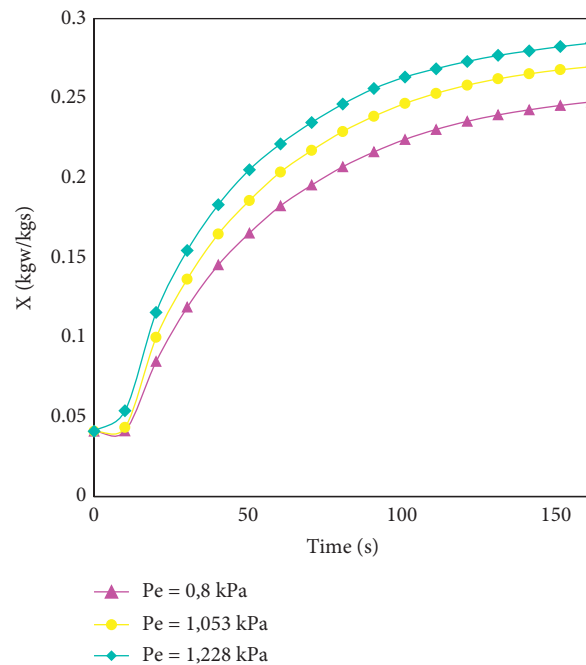


FIGURE 7: Variation of average SAPO-34 uptake with time for different P_e .

difference in the cycle time when the evaporator pressure increases. The duration of the cooling step is totally controlled by the mass transfer rate due to the slow diffusion of water vapor in porous zeolite particles as indicated previously. Enhancement of heat transfer would not have an impact on the cooling step time, the sole way to shorten it is to enhance mass transfer inside porous adsorbent.

It has to be noted that the value of COP given by simulation for a SAPO-34 coated bed (0.622) is close to those of absorption heat pumps (around 0.7); this constitutes a great scientific advancement for adsorption heat pumps

which could place them as serious competing technologies for cooling.

Furthermore, the values of COP and SCP are obtained for an adsorbent heat conductivity of 0.3 W/m K. Higher values are expected to be obtained for higher values of conductivity. In fact, much research and development work is being carried out to enhance heat transfer; one way to achieve that goal is to incorporate within the raw adsorbent additives possessing high conductivities. However, the increase of thermal conductivity could cause the decrease of adsorption capacity and mass transfer rate, so much

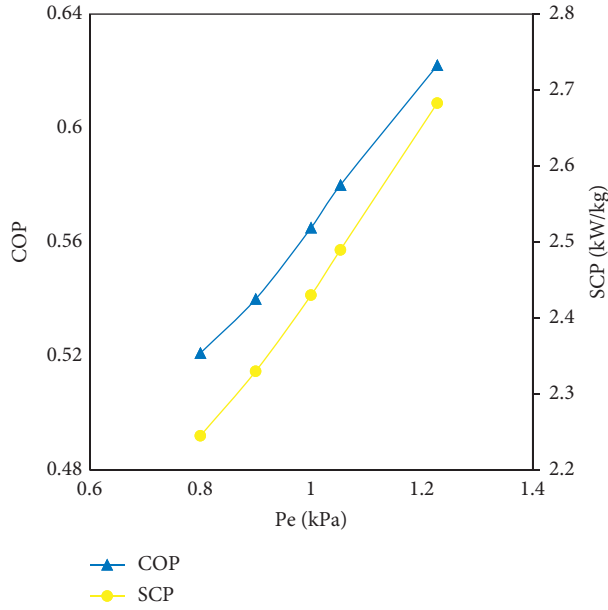


FIGURE 8: Variation of COP and SCP with P_e .

attention is needed when optimizing the preparation of the new adsorbent for heat transfer enhancement. This issue will be addressed in the forthcoming paper.

4. Conclusion

A 2D axisymmetric coupled heat and mass transfer model with initial and boundary conditions was proposed to study a SAPO-34 coated bed.

- (i) The mathematical model has been numerically solved by the use of COMSOL Multiphysics software.

The simulation results agree very well with the experimental data. Furthermore, this study indicates that coated bed is characterized by enhanced heat transfer.

- (ii) Coated bed permits obtaining higher values of COP and SCP compared to granular and consolidated beds. Values of 0.622 for COP and 2.68 kW/kg for SCP can be obtained. Coated beds seem to be well suited for adsorption cooling technologies.

Compared to other approaches like the study proposed and investigated by Melkon Tatlıoer and Ayşe Erdem-Şenatala [50], the SAPO-34 zeolite layer thickness of 0.1 mm can provide a sufficiently high COP value. Furthermore, a good prediction was shown for modeling coated bed by the zeolite SAPO-34 sorbent. Thus, mathematical modeling using COMSOL can provide a useful predictive tool for understanding, design, and optimization of AQSOA-Z02 adsorption/desorption process as an adsorbent material for AHP. This enables us to make significant modifications to avoid damage and failure of the whole designed system.

- (iii) The adsorption heat pump performance is affected by both heat and mass transfer. The enhancement of heat transfer solely is not sufficient to attain high values of COP and SCP. In the case of water vapor/SAPO-34 pair, the mass transfer has a significant impact on the duration of the cooling step which should be shortened if one would want to increase the specific cooling power. The sole way to do it is to enhance mass transfer inside porous adsorbent. The most cited constraints for adsorption heat systems are the huge volume, heavyweight, and high cost. In order to decrease the system's overall volume and weight, several bed configurations can be employed such as finned tube heat exchangers. Therefore, further works on the AHP's is needed to optimize the design of the bed and reduce the model's cost and weight of this study.

Nomenclature

A :	HTF tube surface area, m^2
C_p :	Specific heat, J/kg K
C_{pl} :	Specific heat of liquid water, J/kg K
C_{pv} :	Specific heat of vapor water, J/kg K
COP:	Coefficient of performance
D_{so} :	Reference diffusivity, m^2/s
E :	Characteristics energy, J/mol
E_a :	Activation energy, J/mol
h_i :	Convective heat transfer coefficient between tube and fluid, $W/m^2 K$
h_o :	Wall heat transfer coefficient between tube and adsorbent, $W/m^2 K$
k :	Thermal conductivity, W/m K
L_v :	Latent heat of vaporization, J/kg
m_s :	Mass of sorbent, kg
P :	Pressure, Pa
R :	Universal gas constant, kJ/kmol K
R_v :	Ideal gas constant for vapor, J/kg K
r :	Radial coordinate, m
SCP:	Specific cooling power, kW/kg
T :	Temperature, K
t :	Time, s
T_i :	Initial temperature, K
T_{co} :	Cold fluid inlet temperature, K
T_h :	Hot fluid inlet temperature, K
U :	Vapor velocity vector, m/s
V :	Volume, m^3
X :	Amount of water adsorbed by adsorbent per unit, kg_w/kg_s
z :	Axial coordinate, m
ϵ :	Total porosity
μ :	Dynamic viscosity, kg/m s
ϑ :	Velocity, m/s
κ :	Permeability, m^2
ρ :	Density, kg/m^3
ΔH :	Heat of adsorption, kJ/kg.
<i>Subscripts</i>	
b :	Bed
c :	Condenser

Cyc: Cycle
 e: Evaporator
 f: Fluid
 i: Inner
 l: Lateral
 o: Outer
 p: Particle
 s: Sorbent
 Sat: Saturation
 t: Tube.

Data Availability

The data used to support the findings of this study are included within the article. More supported data can be obtained from the corresponding author upon request.

Conflicts of Interest

The authors declare that they have no conflicts of interest.

Acknowledgments

The authors would like to thank Prof. Luigi Calabrese (Department of Engineering, University of Messina, Italy) and Ms. Valeria Palomba (CNR ITAE in Messina, Italy) for supplying the experimental data.

References

- [1] L. Q. Zhu, C. Y. Tso, K. C. Chan et al., "Experimental investigation on composite adsorbent-water pair for a solar-powered adsorption cooling system," *Applied Thermal Engineering*, vol. 131, pp. 649–659, 2018.
- [2] M. Tatlier and A. Erdem-şenatalar, "The performance analysis of a solar adsorption heat pump utilizing zeolite coatings on metal supports," *Chemical Engineering Communications*, vol. 180, no. 1, pp. 169–185, 2000.
- [3] B. Dawoud, "Water vapor adsorption kinetics on small and full scale zeolite coated adsorbents; A comparison," *Applied Thermal Engineering*, vol. 50, no. 2, pp. 1645–1651, 2013.
- [4] W. Chekirou, R. Boussehain, M. Feidt, A. Karaali, and N. Boukheit, "Numerical results on operating parameters influence for a heat recovery adsorption machine," *Energy Procedia*, vol. 6, pp. 202–216, 2011.
- [5] K. C. A. Alam, B. B. Saha, A. Akisawa, and T. Kashiwagi, "Influence of design and operating conditions on the system performance of a two-stage adsorption chiller," *Chemical Engineering Communications*, vol. 191, Article ID 981997, 2004.
- [6] L. Calabrese, L. Bonaccorsi, P. Bruzzaniti, E. Proverbio, and A. Freni, "SAPO-34 based zeolite coatings for adsorption heat pumps," *Energy*, vol. 187, Article ID 115981, 2019.
- [7] D. Wang, J. Zhang, Q. Yang, N. Li, and K. Sumathy, "Study of adsorption characteristics in silica gel-water adsorption refrigeration," *Applied Energy*, vol. 113, pp. 734–741, 2014.
- [8] D. Wang, J. Zhang, X. Tian, D. Liu, and K. Sumathy, "Progress in silica gel-water adsorption refrigeration technology," *Renewable and Sustainable Energy Reviews*, vol. 30, pp. 85–104, 2014.
- [9] D. C. Wang, Y. H. Li, D. Li, Y. Z. Xia, and J. P. Zhang, "A review on adsorption refrigeration technology and adsorption deterioration in physical adsorption systems," *Renewable and Sustainable Energy Reviews*, vol. 14, no. 1, pp. 344–353, 2010.
- [10] M. S. Fernandes, G. J. V. N. Brites, J. J. Costa, A. R. Gaspar, and V. A. F. Costa, "Review and future trends of solar adsorption refrigeration systems," *Renewable and Sustainable Energy Reviews*, vol. 39, pp. 102–123, 2014.
- [11] L. F. Cabeza, A. Solé, and C. Barreneche, "Review on sorption materials and technologies for heat pumps and thermal energy storage," *Renewable Energy*, vol. 110, pp. 3–39, 2017.
- [12] G. Cacciola and G. Restuccia, "Reversible adsorption heat pump: a thermodynamic model," *International Journal of Refrigeration*, vol. 18, no. 2, pp. 100–106, 1995.
- [13] F. N. Al-Mousawi, R. Al-Dadah, and S. Mahmoud, "Low grade heat driven adsorption system for cooling and power generation with small-scale radial inflow turbine," *Applied Energy*, vol. 183, pp. 1302–1316, 2016.
- [14] M. Schicktanz, K. Thomas Witte, G. Földner, and S. K. Henninger, "Recent developments in adsorption materials and heat exchangers for thermally driven heat pumps," *Research on Working Pairs and Apparatus Technology, Thermally driven heat pumps for heating and cooling*, Universitätsverlag der TU Berlin, Berlin, Germany, 2013.
- [15] S. Santamaria, A. Sapienza, A. Frazzica, A. Freni, I. S. Girnuk, and Y. I. Aristov, "Water adsorption dynamics on representative pieces of real adsorbents for adsorptive chillers," *Applied Energy*, vol. 134, pp. 11–19, 2014.
- [16] Y. I. Aristov, I. S. Glaznev, and I. S. Girnuk, "Optimization of adsorption dynamics in adsorptive chillers: loose grains configuration," *Energy*, vol. 46, no. 1, pp. 484–492, 2012.
- [17] J. J. Guilleminot, A. Choisier, J. B. Chalfen, S. Nicolas, and J. L. Reymoney, "Heat transfer intensification in fixed bed adsorbents," *Heat Recovery Systems and CHP*, vol. 13, no. 4, pp. 297–300, 1993.
- [18] R. Lang, T. Westerfeld, A. Gerlich, and K. F. Knoche, "Enhancement of the heat and mass transfer in compact zeolite layers," *Adsorption*, vol. 2, no. 2, pp. 121–132, 1996.
- [19] G. Restuccia, A. Freni, and G. Maggio, "A zeolite-coated bed for air conditioning adsorption systems: parametric study of heat and mass transfer by dynamic simulation," *Applied Thermal Engineering*, vol. 22, no. 6, pp. 619–630, 2002.
- [20] A. Freni, L. Bonaccorsi, L. Calabrese, A. Capri, A. Frazzica, and A. Sapienza, "SAPO-34 coated adsorbent heat exchanger for adsorption chillers," *Applied Thermal Engineering*, vol. 82, pp. 1–7, 2015.
- [21] S. D. Waszkiewicz, M. J. Tierney, and H. S. Scott, "Development of coated, annular fins for adsorption chillers," *Applied Thermal Engineering*, vol. 29, no. 11–12, pp. 2222–2227, 2009.
- [22] H. Van Heyden, G. Munz, L. Schnabel, F. Schmidt, S. Mintova, and T. Bein, "Kinetics of water adsorption in microporous aluminophosphate layers for regenerative heat exchangers," *Applied Thermal Engineering*, vol. 29, no. 8–9, pp. 1514–1522, 2009.
- [23] A. Freni, A. Frazzica, B. Dawoud, S. Chmielewski, L. Calabrese, and L. Bonaccorsi, "Adsorbent coatings for heat pumping applications: verification of hydrothermal and mechanical stabilities," *Applied Thermal Engineering*, vol. 50, no. 2, pp. 1658–1663, 2013.
- [24] K. Okamoto, M. Teduka, T. Nakano, S. Kubokawa, and H. Kakiuchi, "The Development of AQSOA Water Adsorbent and AQSOA Coated Heat Exchanger," in *Proceedings of the IMPRES conference*, pp. 27–32, Singapore, December 2010.

- [25] H. Demir, M. Mobedi, and S. Ülkü, "A review on adsorption heat pump: problems and solutions," *Renewable and Sustainable Energy Reviews*, vol. 12, no. 9, pp. 2381–2403, 2008.
- [26] H. demir, M. Mobedi, and S. Ülkü, "Heat and mass transfer in the adsorbent bed of an adsorption heat pump," *Chemical Engineering Communications*, vol. 198, pp. 1275–1293, 2011.
- [27] M. Hosseini, F. Farjadian, and S. Hamdy, "Industrial applications for intelligent polymers and coatings," *Industrial Applications for Intelligent Polymers and Coatings*, pp. 1–710, 2016.
- [28] M. Tatlier, "Performances of MOF vs. Zeolite Coatings in Adsorption Cooling Applications," *Applied Thermal Engineering*, vol. 113, 2016.
- [29] G. Restuccia, A. Freni, F. Russo, and S. Vasta, "Experimental Investigation of a Solid Adsorption Chiller Based on a Heat Exchanger Coated with Hydrophobic Zeolite," *Applied Thermal Engineering*, vol. 25, pp. 1419–1428, 2005.
- [30] S. Qian, K. Gluesenkamp, Y. Hwang, R. Radermacher, and Ho-H. Chun, "EnergyEnvironmental impacts of utility-scale solar energy," *Renewable and Sustainable Energy Reviews*, vol. 29, pp. 517–526, 2013.
- [31] L. M. Sun, N. Ben Amar, and F. Meunier, "Numerical study on coupled heat and mass transfers in an absorber with external fluid heating," *Heat Recovery Systems and CHP*, vol. 15, pp. 19–29, 1995.
- [32] A. Çağlar, "The effect of fin design parameters on the heat transfer enhancement in the adsorbent bed of a thermal wave cycle," *Applied Thermal Engineering*, vol. 104, pp. 386–393, 2016.
- [33] L. Z. Zhang, "A three-dimensional non-equilibrium model for an intermittent adsorption cooling system," *Solar Energy*, vol. 69, pp. 27–35, 2000.
- [34] A. Pesaran, H. Lee, Y. Hwang, R. Radermacher, and H. H. Chun, "Review article: numerical simulation of adsorption heat pumps," *Energy*, vol. 100, pp. 310–320, 2016.
- [35] A. Çağlar, C. Yamali, and D. K. Baker, "Two-dimensional transient coupled analysis of a finned tube adsorbent bed for a thermal wave cycle," *International Journal of Thermal Sciences*, vol. 73, pp. 58–68, 2013.
- [36] M. W. Ellis, "Effects of adsorbent conductivity and permeability on the performance of a solid sorption heat pump," *Journal of Energy Resources Technology*, vol. 121, pp. 51–59, 1999.
- [37] S. İsmail, D. A. S. Rees, C. Yamali, D. Basker, and B. Kaftanoğlu, "Numerical investigation of coupled heat and mass transfer inside the adsorbent bed of an adsorption cooling unit," *International Journal of Refrigeration*, vol. 35, pp. 652–662, 2012.
- [38] I. Solmuş, C. Yamali, C. Yildirim, and K. Bilen, "Transient behavior of a cylindrical adsorbent bed during the adsorption process," *Applied Energy*, vol. 142, pp. 115–124, 2015.
- [39] R. H. Mohammed, O. Mesalhy, M. L. Elsayed, and L. C. Chow, "Performance evaluation of a new modular packed bed for adsorption cooling systems," *Applied Thermal Engineering*, vol. 136, 2017.
- [40] P. G. Youssef, S. M. Mahmoud, and R. K. Al-Dadah, "Effect of evaporator temperature on the performance of water desalination/refrigeration adsorption system using AQSOA-ZO2," *International Journal of Environmental, Chemical, Ecological, Geological and Geophysical Engineering*, vol. 9, no. 6, 2015.
- [41] M. Syed and A. Chakraborty, "Adsorption assisted double stage cooling and desalination employing silica gel + water and AQSOA-ZO2 + water systems," *Energy Conversion and Management*, vol. 117, pp. 193–205, 2016.
- [42] S. Kayal, S. Baichuan, and B. Baran, "International journal of heat and mass transfer adsorption characteristics of AQSOA zeolites and water for adsorption chillers," *International Journal of Heat and Mass Transfer*, vol. 92, pp. 1120–1127, 2016.
- [43] B. B. Saha, K. Uddin, A. Pal, and K. Thu, "Emerging sorption pairs for heat pump applications: an overview," *JMST Advances*, vol. 1, pp. 161–180, 2019.
- [44] Y. Liu and K. C. Leong, "Numerical study of a novel cascading adsorption cycle," *International Journal of Refrigeration*, vol. 29, pp. 250–259, 2006.
- [45] M. H. Chahbani, J. Labidi, and J. Paris, "Effect of mass transfer kinetics on the performance of adsorptive heat pump systems," *Applied Thermal Engineering*, vol. 22, no. 1, pp. 23–40, 2002.
- [46] M. Intini, M. Goldsworthy, S. White, and C. M. Joppolo, "Experimental analysis and numerical modelling of an AQSOA zeolite desiccant wheel," *Applied Thermal Engineering*, vol. 80, pp. 20–30, 2015.
- [47] I. S. Girnîk and Y. I. Aristov, "Making adsorptive chillers faster and more efficient: the effect of bi-dispersed adsorbent bed," *Applied Thermal Engineering*, vol. 106, pp. 254–256, 2016.
- [48] U. Wittstadt, G. Fuldner, O. Andersen, R. Herrmann, and F. Schmidt, "A new adsorbent composite material based on metal fiber technology and its application in adsorption heat exchangers," *Energies*, vol. 8, pp. 8431–8446, 2015.
- [49] C. McCague, W. Huttema, A. Fradin, and M. Bahrami, "Lab-scale sorption chiller comparison of FAM-ZO2 coating and pellets," *Applied Thermal Engineering*, vol. 173, 2020.
- [50] M. Tatlıoer and A. Erdem-Şenatala, "Effects of metal mass on the performance of adsorption heat pumps utilizing zeolite 4A coatings synthesized on heat exchanger tubes," *International Journal of Refrigeration*, vol. 23, pp. 260–268, 2000.